Optical visualization and quantification of enzyme activity using dynamic droplet lenses

Lauren D. Zarzar[a,b,1], Julia A. Kalow[a,b,2], Xinping He[a,b,3], Joseph J. Walish[a,b], and Timothy M. Swager[a,b,4]

[a]Department of Chemistry, Massachusetts Institute of Technology, Cambridge, MA 02139; and [b]Institute for Soldier Nanotechnologies, Massachusetts Institute of Technology, Cambridge, MA 02139

Edited by David A. Weitz, Harvard University, Cambridge, MA, and approved March 7, 2017 (received for review November 14, 2016)

In this paper, we describe an approach to measuring enzyme activity based on the reconfiguration of complex emulsions. Changes in the morphology of these complex emulsions, driven by enzyme-responsive surfactants, modulate the transmission of light through a sample. Through this method we demonstrate how simple photodetector measurements may be used to monitor enzyme kinetics. This approach is validated by quantitative measurements of enzyme activity for three different classes of enzymes (amylase, lipase, and sulfatase), relying on two distinct mechanisms for coupling droplet morphology to enzyme activity (host–guest interactions with uncaging and molecular cleavage).

emulsion | enzyme | assay | sensor | lenses

Bioassays are used extensively in healthcare for the identification and quantification of biochemical markers, such as enzymes, which have long been known to be important diagnostic indicators for monitoring many diseases and health states. Tests indicating abnormal enzyme activity, in combination with physical examination, are used to diagnose many illnesses, such as pancreatitis (lipase and amylase) (1), myocardial infarction (creatine kinase) (2), and liver disease (aspartate aminotransferase, alanine aminotransferase, alkaline phosphatase) (3). Rather than quantify the concentration of these enzymes directly, clinicians usually monitor the production or consumption of an enzyme's substrate. Conventionally, clinical samples are tested by professional laboratories with specialized commercial equipment, and these assays often rely on a colorimetric or fluorogenic signal generated by enzyme action. Historically, reagent and equipment requirements for these assays have limited their use to professional laboratories in developed nations. The creation of point-of-care diagnostics which will enable rapid, low-cost, and personalized healthcare options offers the ability to improve the well-being of people, especially in developing countries (4, 5). Such recent advances include development of portable quantum dot microspectrometer technology (6), paper-based bioassays (7), handheld portable devices for virus particle sizing using nanolenses (8), and smartphone-powered multiplex ELISAs (9). The emergence of smartphone-driven personal health monitoring (9–11) in particular creates a market for scalable, easily executed, inexpensive assays that harness built-in smartphone components (camera, light sensor, magnetometer, etc.) and automate interpretation. The continued development of conceptually novel approaches to bioassays, especially for enzymes, will be critical for the ongoing advancement of point-of-care technology and low-cost health monitoring.

Stimuli-responsive "smart" materials have the ability to enable new diagnostic devices that expand the suite of sensitivities and readout mechanisms for point-of-care platforms (12). Recently, we described a facile approach to the fabrication of reconfigurable complex droplets (13) that, because of their exquisitely sensitive morphological response to targeted chemical stimuli, have significant promise as an easily deployable liquid-sensing platform. Using our method, complex droplets can be produced from two immiscible liquids: a fluorinated liquid (F) and a hydrocarbon or organic liquid (H) dispersed within an outer aqueous phase containing surfactants. The low interfacial tension between the hydrocarbon and fluorocarbon phases (γ_{FH}) creates dynamic complex droplet morphologies that respond to minute changes in the balance of interfacial tensions at the water–fluorocarbon interface (γ_F) and the water–hydrocarbon interface (γ_H). The droplets assume a double-emulsion hydrocarbon-in-fluorocarbon-in-water (H/F/W) morphology when ($\gamma_H >> \gamma_F$), a Janus morphology when ($\gamma_H \sim \gamma_F$), and a double-emulsion F/H/W morphology when ($\gamma_H << \gamma_F$) (Fig. 1*A*). Changes in the droplet morphology are triggered by altering surfactant concentrations or surfactant effectiveness, and examples of the latter include stimuli-responsive or cleavable surfactants (13).

It was recently demonstrated that complex droplets have usefulness as responsive lenses (Fig. 1*A*) and the morphology determines the droplets' optical refractory properties (14). Optical changes caused by variations in droplet morphology are visible to the naked eye and provide an optical readout mechanism for droplet shape. For instance, layers of double emulsions are opaque, whereas Janus droplets are transmissive, which is a function of both the droplet shape and the liquids' index of refraction (Fig. 1*B*). Considering that complex droplets can now be produced by facile scalable methods, and an optical scattering sensing mechanism is elegant in its simplicity, we have explored responsive droplet lenses as a new technology for implementing a low-cost, point-of-care platform able to sense a wide range of diagnostic molecules.

We report herein a broadly applicable enzyme-sensing assay predicated on the optical changes of enzyme-responsive complex droplet lenses. We present two approaches by which to couple enzyme activity to the droplet morphology: enzyme uncaging of a surfactant and enzyme-degradable surfactants. We demonstrate that changes in the optical transmission of the droplet lenses are sufficient for quantification of α-amylase, lipase, and sulfatase activity and that the transmission data can be collected either with a spectrometer or with a personal electronic device such as a smartphone or tablet. Given the highly generalizable nature of this sensing platform as well as its simplicity, we believe this dynamic droplet lens sensor approach can be extended to other enzyme classes as well as for enzyme-linked assays.

Significance

A nonfluorescence-based technology is introduced that can lead to visual detection of enzyme activity. These results represent a dramatically different paradigm for creating sensors based on dynamic liquid lenses with general utility.

Author contributions: L.D.Z., J.A.K., and T.M.S. designed research; L.D.Z., J.A.K., X.H., and J.J.W. performed research; L.D.Z., J.A.K., and T.M.S. analyzed data; and L.D.Z., J.A.K., and T.M.S. wrote the paper.

The authors declare no conflict of interest.

This article is a PNAS Direct Submission.

[1]Present address: Department of Materials Science and Engineering and Department of Chemistry, The Pennsylvania State University, University Park, PA 16802.

[2]Present address: Department of Chemistry, Northwestern University, Evanston, IL 60208.

[3]Present address: Department of Chemical Engineering, Tianjin University, Tianjin 300072, People's Republic of China.

[4]To whom correspondence should be addressed. Email: tswager@mit.edu.

This article contains supporting information online at www.pnas.org/lookup/suppl/doi:10.1073/pnas.1618807114/-/DCSupplemental.

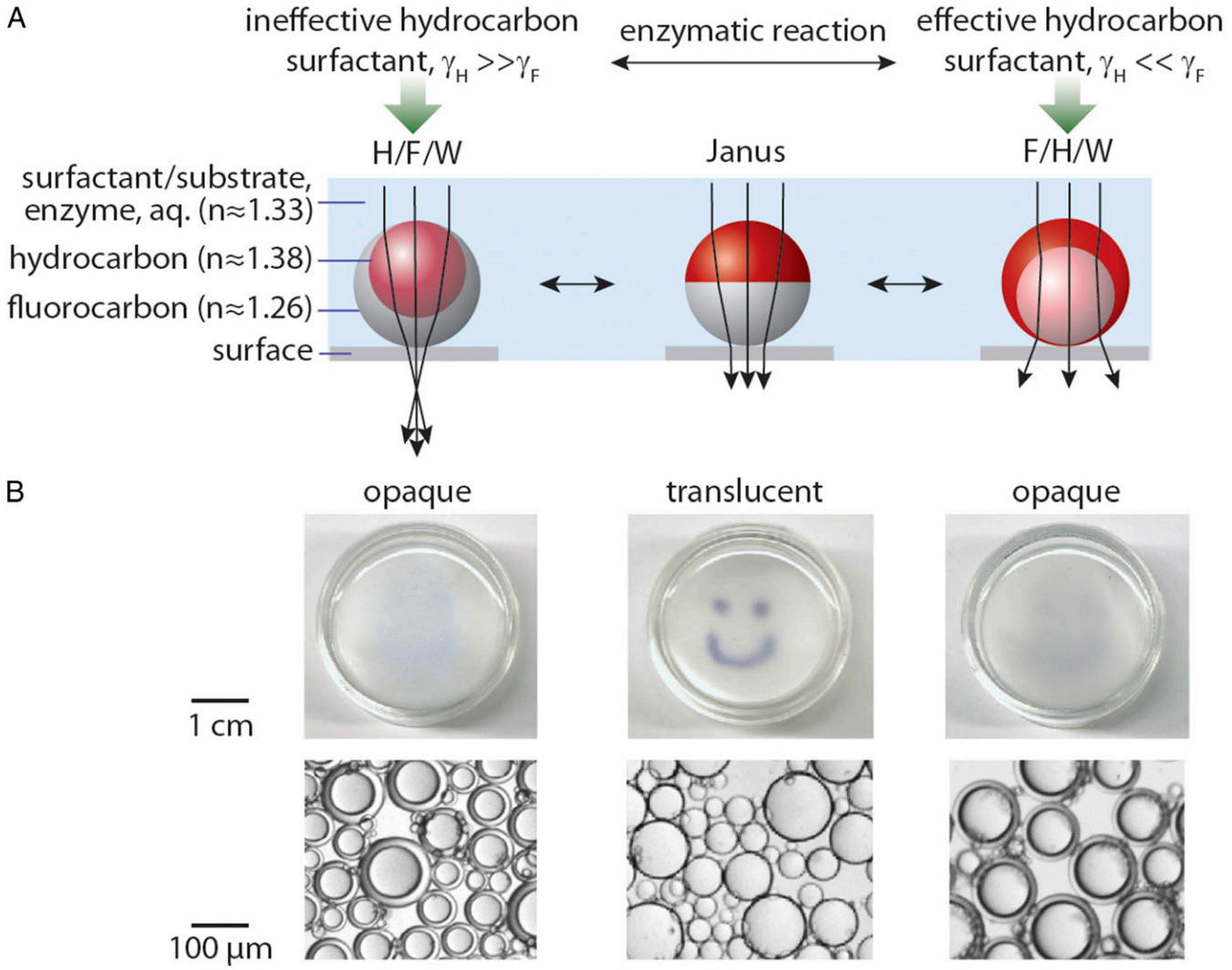

Fig. 1. Reconfigurable droplets act as tunable lenses and the optical transmission of an emulsion film depends on the droplet morphology. (*A*) Schematic ray diagrams of the complex droplets composed of hydrocarbon (e.g., hexane, heptane) and fluorocarbon (e.g., perfluorohexane, FC770) within a continuous phase of aqueous solution containing the enzyme and substrate/surfactant. Approximate refractive indices are given. Depending on the surfactant conditions and the interfacial tensions at the fluorocarbon–water (γ_F) and hydrocarbon–water (γ_H) interfaces, these droplets dynamically change their morphology and can adopt three general configurations: H/F/W, Janus, or F/H/W. We note that depending on the specific refractive indices of liquids used, the most transmissive Janus drop may not be the precise morphology as pictured (where $\gamma_F = \gamma_H$) but may be a Janus drop with slight curvature at the fluorocarbon–hydrocarbon interface. Because fluorinated liquids have a greater density, the droplets orient with gravity when sitting on a surface, which is important to achieving the desired optical response. (*B*) Aligned beneath the droplet schematics are corresponding photographs of polydisperse emulsions in a Petri dish placed over an image of a happy face to demonstrate changes in the optical transmission. (Scale, 1 cm.) Pictured below are optical micrographs of representative droplets. (Scale, 100 μm.)

Results

Determination of α-Amylase Activity via Disruption of Host–Guest Interactions. To determine whether the reconfiguration of the droplet lenses can be used to measure enzyme activity, we began with an emulsion system sensitive to the activity of α-amylase. α-Amylase, an enzyme that catalyzes the hydrolytic cleavage of internal α-1,4-glycosidic linkages in polysaccharides, is an important diagnostic enzyme and relevant biomarker for many gastrointestinal tract conditions. The ability of amylase to affect surface tensions by disrupting host–guest complexes between cyclodextrins and surfactants has previously been explored (15), making it an excellent model system to test the proposed sensing scheme. We used α-amylase from *Aspergillus oryzae* as the enzyme, and we chose γ-cyclodextrin (γ-CD) as the enzyme substrate because it forms a 1:1 inclusion complex with Triton X-100 surfactant (16) and the larger γ-CD is enzymatically degraded more rapidly (with a higher V_{max}) than the smaller α- and β-CD (17).

To sensitize the droplets to the amylase enzyme, we prepared droplets in an aqueous sodium acetate (NaOAc) buffered solution containing a bound (caged) hydrocarbon surfactant (Triton X-100/γ-CD) and an inert fluorosurfactant, Zonyl FS-300 (Zonyl) (Fig. 2*A*). Droplets were composed of heptane and FC770 (a mixed fluorocarbon solvent) in a 1:1 volume ratio. Droplets experiencing this Triton X-100/γ-CD complex in conjunction with Zonyl surfactant exhibited an H/F/W morphology, revealing that the surfactant effectiveness of the Triton X-100 is compromised when complexed with γ-CD (16). Upon introduction of α-amylase, hydrolysis of the γ-CD "uncages" the Triton X-100 molecules and triggers a change in the balance of interfacial tensions. Over time, droplets transitioned through a Janus morphology and finally assumed an F/H/W droplet morphology that is favored by a stabilization of the hydrocarbon water interface ($\gamma_H << \gamma_F$) by liberated Triton X-100.

To demonstrate that the droplet shape could be a useful indicator in a quantitative assay, we investigated the rate of change

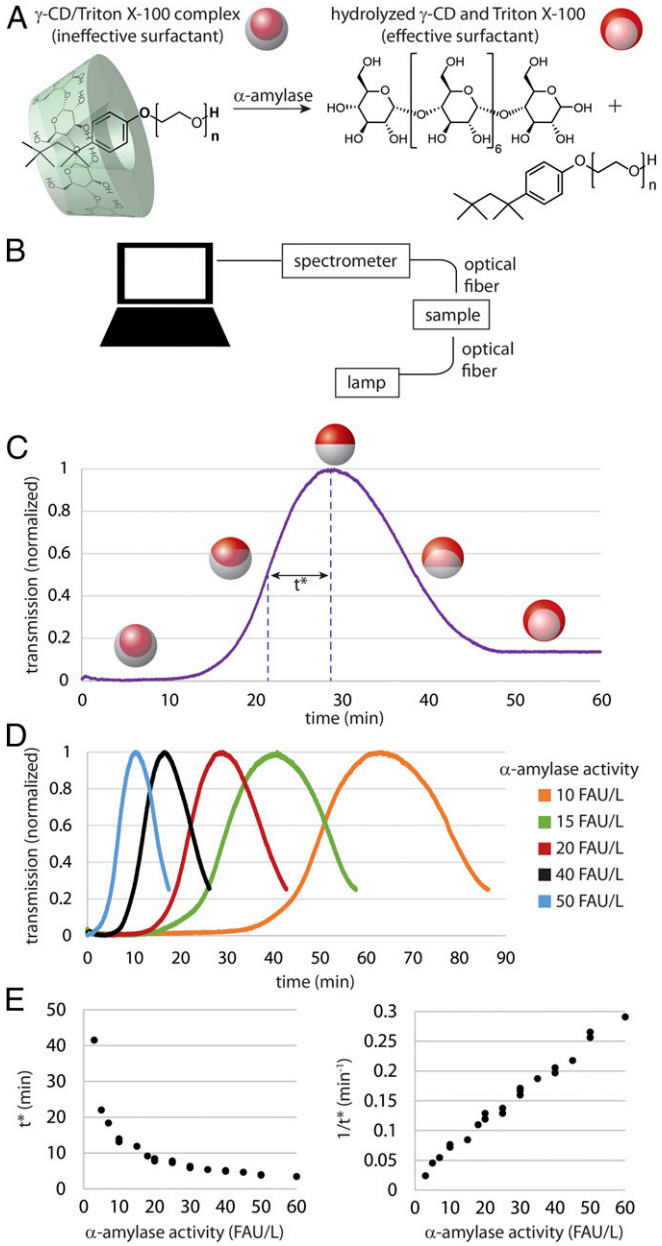

Fig. 2. Measurement of α-amylase activity using variations in transmission of responsive droplet lenses. (*A*) When Triton X-100 surfactant is complexed with γ-CD it is no longer an effective surfactant, and droplets in the presence of this Triton X-100/ γ-CD complex along with Zonyl fluorosurfactant exhibit H/F/W morphology. When the γ-CD is hydrolyzed by α-amylase, the Triton X-100 becomes freely available, thereby reducing γ_H relative to γ_F and pushing the droplets closer toward the F/H/W state. (*B*) Schematic of the experimental setup; a stabilized light source was used for illumination and a USB spectrometer was used to measure the intensity of transmitted 650-nm light. (*C*) Exemplary transmission versus time data collected for a sample with 20 FAU/L α-amylase activity. Droplets began in the opaque H/F/W state, transitioned through the transmissive Janus state, and ended in an F/H/W configuration. We define t* to equal the time difference between when maximum and half-maximum transmission is reached. (*D*) Exemplary transmission versus time plots for varying concentrations of amylase all using the same reaction scheme shown in *B*. Data were collected at 37 °C. (*E*) The time parameter t* was determined for 22 independent samples across a range of relevant amylase activities (*Left*). The rate of the reaction, characterized by 1/t*, is plotted versus amylase activity and yields a linear correlation with $R^2 = 0.989$ (*Right*).

in the droplet morphology with respect to enzyme activity. Given the previously established relationship between a droplet's shape and its optical properties (14), we chose to use macroscale optical transmission measurements as an indicator of the droplet morphology rather than direct imaging of the droplets themselves in a microscope. We measured the optical transmission at 650 nm through a glass-bottom dish (*SI Appendix*, Fig. S1) containing several layers of microscale polydisperse droplets using a spectrometer and a stabilized tungsten light source in an incubator at 37 °C (Fig. 2*B*). The transmission intensity was tracked over time for a sample containing a known α-amylase activity, defined in fungal α-amylase units (FAU) per liter (Fig. 2*C*). Droplets began in an opaque H/F/W double-emulsion morphology, transitioned through the translucent Janus morphology, and finally ended in an opaque F/H/W morphology, as expected.

To quantitatively describe the transmission curve and provide a basis for comparison between samples, we defined a time parameter t* to be equal to the time difference between maximum and half-maximum transmission. Effectively, t* is a measure of how long it takes for the droplets to change between two specific morphologies (Fig. 2*C*). The amount of degraded γ-CD (which is directly related to the amount of liberated Triton X-100) correlates to the droplet shape and as a result, measuring t* is equivalent to measuring the amount of time required for the enzyme to process a defined amount of substrate. Following this paradigm, we subjected droplets to a range of varying α-amylase activities (Fig. 2*D*), observing that with higher α-amylase activity, the change in droplet morphology occurs more quickly, resulting in a smaller t* (Fig. 2*E*, *Left*). A plot of 1/t* (representing the rate at which the γ-CD is degraded) vs. known enzyme activity yielded a linear calibration curve (Fig. 2*E*, *Right*).

Determination of Lipase and Sulfatase Activity via Direct Surfactant Degradation. Having demonstrated a proof-of-concept assay for α-amylase via uncaging of a surfactant, we next explored assays for lipase activity based on direct enzymatic cleavage of a surfactant. Lipase is an important diagnostic enzyme and biomarker for conditions involving the pancreas, such as pancreatitis. We used lipase from *Candida* sp. as the enzyme, tetra(ethylene glycol)mono-*n*-octanoate (**1**) as the lipase-degradable hydrocarbon surfactant (18), and Zonyl as the inert fluorinated surfactant within PBS solution (Fig. 3*A*). Droplets were composed of a 1:1 volume ratio of (2:1 hexane:heptane) and perfluorohexane. Experiments were conducted at room temperature (20–21 °C) with the same spectrometer configuration as used for the α-amylase measurements. In this case, droplets exhibited the reverse morphology trajectory compared with the α-amylase scheme. Specifically, when degraded by lipase, the surfactant (**1**) is transformed into a molecule that is an ineffective surfactant and droplets transitioned to the H/F/W state over time (Fig. 3*B*). Nevertheless, the same definition of t*, as was used in the amylase assay, remains applicable. Exemplary linear transmission versus time curves are shown in Fig. 3*C* and the correlation between t* and 1/t* with lipase activity as expressed in lipase units (LU) is shown in Fig. 3*D*. Control experiments that hinder catalytic activity of lipase with a covalent inhibitor, methyl 4-nitrophenyl hexylphosphonate, resulted in neither change in droplet shape nor change in transmission, confirming that variations in droplet morphology are a direct result of the lipase activity and not from hydrolysis of the surfactant over time in aqueous solution (*SI Appendix*, Fig. S2).

Using a similar surfactant-degradation approach, we next designed a system responsive to sulfatase. Sulfatases hydrolyze sulfate esters found on steroids, carbohydrates, and proteins. Extracellular sulfatases are up-regulated in some tumors, whereas sulfatase deficiency is associated with lysosomal storage diseases (19–21). Novel fluorogenic probes for bacterial sulfatase activity, which occurs at a distinct pH range compared with

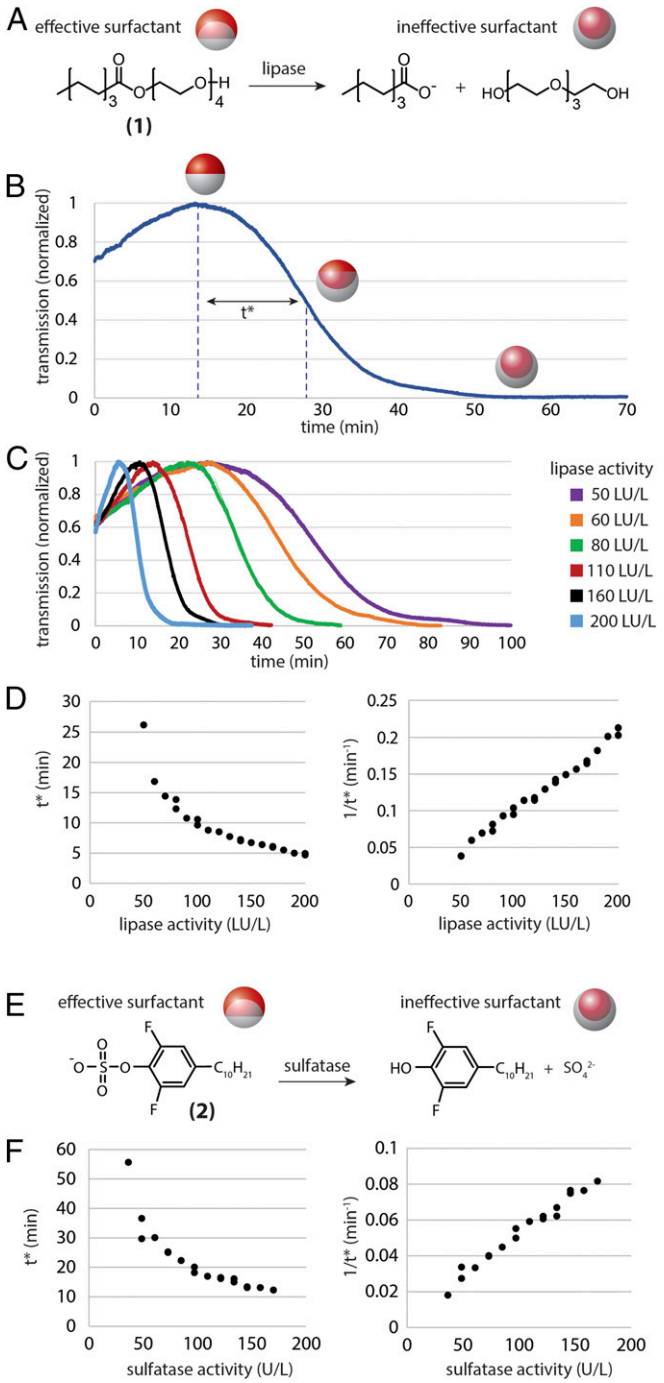

Fig. 3. Measurement of lipase and sulfatase activity via direct enzymatic degradation of surfactants. (*A*) Droplets in the presence of an ester-linked surfactant (**1**) and Zonyl initially exhibit a Janus-type morphology. When the ester-linked surfactant is hydrolyzed by lipase, γ_H increases relative to γ_F and the droplets transition toward the H/F/W state. (*B*) Exemplary transmission versus time plot for emulsions sensitized by the lipase-responsive surfactants shown in *A* at 70 LU/L. Although the droplets follow the reverse trajectory as demonstrated in Fig. 2, we can still apply the same definition of t*. (*C*) Transmission versus time plots for samples containing varying concentrations of lipase and using the reaction scheme shown in *A*. Data were collected at 21 °C. (*D*) The time parameter t* was determined for 22 independent samples across a range of relevant lipase activities (*Left*). The rate of the reaction, characterized by 1/t*, is plotted versus lipase activity and yields a linear correlation with R^2 = 0.99 (*Right*). (*E* and *F*) Measurement of sulfatase activity. (*E*) Droplets in the presence of sulfate surfactant (**2**) and Zonyl initially exhibit a Janus-type morphology. When the sulfate surfactant is hydrolyzed by sulfatase, γ_H increases relative to γ_F and the droplets transition toward the H/F/W state. (*F*) The time parameter t* was determined for 18 independent samples across a range of sulfatase activities (*Left*). The rate of the reaction, characterized by 1/t*, is plotted versus sulfatase activity and yields a linear correlation with R^2 = 0.977 (*Right*). Data were collected at 37 °C.

mammalian sulfatases, have enabled the rapid discrimination of tuberculosis strains (22, 23). The mechanism for droplet reconfiguration in the sulfatase assay is analogous to the lipase scheme. In particular, sulfatase-cleavable surfactant 4-decyl-2,6-difluorophenyl sulfate (**2**) was used along with inert Zonyl fluorosurfactant and sulfatase from *Helix pomatia* in sodium acetate buffer (Fig. 3*E*). The droplets were composed of a 1:1 volume ratio of heptane and FC770, and measurements were again collected in an incubator at 37 °C. The calculated t* values for various sulfatase activities and the corresponding rates (1/t*) are shown in Fig. 3*F*, where 1 unit is defined as the amount of enzyme that can hydrolyze 1.0 μmol of *p*-nitrocatechol sulfate per hour at pH 5 and 37 °C. We again observed a linear correlation between 1/t* and enzyme activity.

Enzyme Sensing with a Personal Electronic Device. To explore the possibility that such dynamic droplet lenses could potentially be useful in field experiments and for point-of-care diagnostics, we aimed to demonstrate that such droplet transmission data could be easily collected with commonplace equipment. Our initial experiments with lipase, amylase, and sulfatase were all conducted with a spectrometer, computer software data collection, and an intensity-stabilized light source. This equipment provided the necessary precision for the initial elucidation of the droplet response and activity correlation, but are expensive and impractical for low-cost point-of-care diagnostics. Because all that is required for the proposed assay scheme is the tracking of light intensity over time, we investigated if the light sensors that are now standard equipment on personal electronic devices such as camera phones or tablets could be used in place of the spectrometer and computer. Using the free Physics Toolbox Light Sensor Android application on a Samsung Note tablet 2014 Edition (model SM-P600) and the ambient fluorescent room lighting for illumination, we collected light-transmission versus time data for an exemplary sample, 200 LU/L lipase at room temperature (20 °C) (Fig. 4). Although the light sensor lacks the precision of the spectrometer and so the intensity measurements are more discretized, the overall shape of the curve is nearly equivalent with the data shown in Fig. 3*B* and still allows determination of t*. A fieldable tablet or phone-based assay will still require some development and standardization, but nevertheless the fact that simple measurement of light intensity appears sufficient for application of this assay is promising for the development of low-cost point-of-care diagnostics.

Discussion

We tested the proposed droplet lens assay scheme with three different enzymes (α-amylase, lipase, and sulfatase) and two different sensitizing mechanisms (host–guest disruption or uncaging and surfactant cleavage). The results in all three cases suggest that the enzyme activity is strongly correlated with the defined time parameter t*, which is easily quantifiable based on changes in optical transmission of droplet films. The correlation between the rate of droplet morphology change (as expressed by 1/t*) and enzyme activity is linear, suggesting that the kinetics are apparent zero order with respect to substrate concentration and first order with respect to enzyme activity, desirable for enzyme assays. This linear relationship is expected to be general for all enzymes in their Michaelis–Menten zero-order regime. Thus, it appears that our measured values of 1/t* are equivalent in function to traditional enzyme unit measurements, but may be determined using simple transmission measurements with droplet

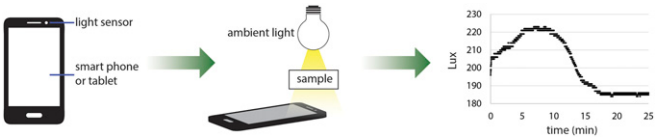

Fig. 4. Portable electronic devices such as smartphones and tablets have light sensors that can be used along with ambient lighting conditions to collect enzyme activity data similar to that achieved using a spectrometer and a computer. The data shown at right were collected for 200 U/L lipase at 21 °C using a Samsung tablet.

lenses. The results also indicate that the presence of the chosen surfactants in the solution does not interfere significantly with the enzyme activity.

We anticipate that the time required for the assay, which is closely related to the kinetics of the enzyme–substrate interactions, can be tuned by rational design of the substrate. We used such an approach to begin to optimize the sulfatase substrate (*SI Appendix*, Fig. S3) and used a lipase-degradable surfactant that had previously undergone preliminary optimization by Stjerndahl and Holmberg (24). Future work on the molecular design of the substrate may allow for generation of even more rapid diagnostics. We do note however that the rate of change in droplet morphology is not purely based on the enzyme reaction rates but also depends on how quickly surfactant molecules adsorb and desorb from the interface, as well as on the rate of diffusion of molecules to the droplet interface. For this reason, we point out that we specifically chose to measure enzyme activities where t* was on the order of at least a few minutes so that diffusion was not rate limiting. Typically, enzymes are not present in high concentrations and dilution is always possible, so we do not anticipate this to be a significant limitation for these assays.

For point-of-care and rapid diagnostics, another important consideration is the shelf life of the assay as well as ease of high-throughput or automated readout. Indeed, we are using liquid droplets which are not stable indefinitely and eventually will succumb to coalescence, even if over the timeframe of months or longer. However, we emphasize two characteristics of this approach that provide this droplet assay with relatively longer shelf life and greater ease of use. First, this assay works with droplets that are polydisperse, and so even if some coalescence occurs, the resulting size change would not significantly affect the results. Second, these droplets can be fabricated in bulk volumes with a simple procedure (13) that can be conducted at the time of use if needed. We also envision that this assay would be compatible with high-throughput readout mechanisms; integration with multiwell plate readers would allow measurement of tens to hundreds of samples at once by an automated machine, greatly expanding ease of use and throughput.

Conclusions

The generation of simple, portable, low-cost diagnostic devices is of increasing importance for the developing world as well as for personal healthcare monitoring. The ability to quantify enzyme activity is critical, both for the direct determination of the activity of specific diagnostically relevant enzymes, but also for use in enzyme-linked assay platforms. We have described here an assay predicated on the optical changes of enzyme-responsive complex droplets and demonstrated that optical transmission measurements can be used to quantitatively describe the activity of α-amylase, lipase, and sulfatase in solution. We demonstrated two approaches by which to sensitize the droplets using host–guest interactions and enzyme-degradable surfactants. However, there are many other viable routes for the creation of responsive surfactants and amphiphiles (25), including oxidation/reduction reactions, isomerization, or phosphorylation. Given the ease of droplet fabrication and the simplicity of the optical sensing method, we believe that these dynamic droplets have significant potential as a broadly deployable biosensing platform.

ACKNOWLEDGMENTS. We thank Professor Ellen M. Sletten for helpful discussions. This work was supported by the Army Research Office through the Institute for Soldier Nanotechnologies. J.A.K. was supported by a F32 Ruth L. Kirschstein National Research Service Award Fellowship under Award GM106550. X.H. acknowledges the Internship Program of Tianjin University in World-leading Universities for financial support.

1. Sternby B, O'Brien JF, Zinsmeister AR, DiMagno EP (1996) What is the best biochemical test to diagnose acute pancreatitis? A prospective clinical study. *Mayo Clin Proc* 71: 1138–1144.
2. Novis DA, Jones BA, Dale JC, Walsh MK; College of American Pathologists (2004) Biochemical markers of myocardial injury test turnaround time: A College of American Pathologists Q-Probes study of 7020 troponin and 4368 creatine kinase-MB determinations in 159 institutions. *Arch Pathol Lab Med* 128:158–164.
3. Reichling JJ, Kaplan MM (1988) Clinical use of serum enzymes in liver disease. *Dig Dis Sci* 33:1601–1614.
4. Kumar AA, et al. (2015) From the bench to the field in low-cost diagnostics: Two case studies. *Angew Chem Int Ed Engl* 54:5836–5853.
5. Gubala V, Harris LF, Ricco AJ, Tan MX, Williams DE (2012) Point of care diagnostics: Status and future. *Anal Chem* 84:487–515.
6. Bao J, Bawendi MG (2015) A colloidal quantum dot spectrometer. *Nature* 523:67–70.
7. Martinez AW, Phillips ST, Butte MJ, Whitesides GM (2007) Patterned paper as a platform for inexpensive, low-volume, portable bioassays. *Angew Chem Int Ed Engl* 46:1318–1320.
8. McLeod E, et al. (2015) High-throughput and label-free single nanoparticle sizing based on time-resolved on-chip microscopy. *ACS Nano* 9:3265–3273.
9. Laksanasopin T, et al. (2015) A smartphone dongle for diagnosis of infectious diseases at the point of care. *Sci Transl Med* 7:273re1.
10. Rodriguez-Manzano J, et al. (2016) Reading out single-molecule digital RNA and DNA isothermal amplification in nanoliter volumes with unmodified camera phones. *ACS Nano* 10:3102–3113.
11. Bates M, Zumla A (2015) Rapid infectious diseases diagnostics using Smartphones. *Ann Transl Med* 3:215.
12. Verma R, Adhikary RR, Banerjee R (2016) Smart material platforms for miniaturized devices: Implications in disease models and diagnostics. *Lab Chip* 16:1978–1992.
13. Zarzar LD, et al. (2015) Dynamically reconfigurable complex emulsions via tunable interfacial tensions. *Nature* 518:520–524.
14. Nagelberg S, et al. (2017) Reconfigurable and responsive droplet-based compound micro-lenses. *Nat Commun* 8:14673.
15. Jiang L, Yan Y, Drechsler M, Huang J (2012) Enzyme-triggered model self-assembly in surfactant-cyclodextrin systems. *Chem Commun (Camb)* 48:7347–7349.
16. Saito Y, Ueda H, Abe M, Sato T, Christian SD (1998) Inclusion complexation of triton X-100 with α-, β- and γ-cyclodextrins. *Colloids Surf, A* 135:103–108.
17. Jodái I, Kandra L, Harangi J, Nánási P, Szejtli J (1984) Hydrolysis of cyclodextrin by Aspergillus oryzae α-amylase. *Starke* 36:140–143.
18. Stjerndahl M, van Ginkel CG, Holmberg K (2003) Hydrolysis and biodegradation studies of surface-active esters. *J Surfactants Deterg* 6:319–324.
19. Diez-Roux G, Ballabio A (2005) Sulfatases and human disease. *Annu Rev Genomics Hum Genet* 6:355–379.
20. Morimoto-Tomita M, et al. (2005) Sulf-2, a proangiogenic heparan sulfate endosulfatase, is upregulated in breast cancer. *Neoplasia* 7:1001–1010.
21. Nawroth R, et al. (2007) Extracellular sulfatases, elements of the Wnt signaling pathway, positively regulate growth and tumorigenicity of human pancreatic cancer cells. *PLoS One* 2:e392.
22. Beatty KE, et al. (2013) Sulfatase-activated fluorophores for rapid discrimination of mycobacterial species and strains. *Proc Natl Acad Sci USA* 110:12911–12916.
23. Rush JS, Beatty KE, Bertozzi CR (2010) Bioluminescent probes of sulfatase activity. *ChemBioChem* 11:2096–2099.
24. Stjerndahl M, Holmberg K (2003) Synthesis and chemical hydrolysis of surface-active esters. *J Surfactants Deterg* 6:311–318.
25. Kang Y, Tang X, Cai Z, Zhang X (2016) Supra-amphiphiles for functional assemblies. *Adv Funct Mater* 26:8920–8931.